NOVA SYMMETRY: EXPERIMENTS, MODELING, AND INTERPRETATION (HLP3 AND HLP4)

L. J. Suter *N. Delameter*[*] *E. K. Lindman**
A. A. Hauer[*] *S. G. Glendinning* *A. R. Thiessen*
L. V. Powers *W. W. Hsing*[*] *R. E. Turner*
D. B. Ress *O. L. Landen*

Introduction

Understanding and controlling capsule implosion symmetry is a key requirement for inertial confinement fusion (ICF). Symmetry was specifically called out in the Nova Technical Contract (NTC) as the HLP4 task. Later, elements of HLP3 were expanded to include symmetry work. For nearly a decade and a half it has been recognized that the fundamental asymmetry in a laser-heated hohlraum is a long-wavelength pole-waist radiation flux variation[1] that varies like the P_2 Legendre polynomial.[2] It has also been recognized that we can control this asymmetry and achieve nearly symmetric implosions by appropriately pointing the laser beams.[3]

Review of Symmetry in Hohlraums

To understand symmetry in hohlraums, consider a cylindrically shaped, Nova-like hohlraum with beams aimed as shown in Fig. 1(a). An observer at the capsule location would see a collimated source flux vs angle approximately as shown in the flux vs polar angle plot. The laser-produced hot spot causes a peak in this source at ~60° polar angle. The cold, nonemitting laser entrance hole (LEH) provides zero flux at low polar angle. If we resolve this source flux vs angle into its Legendre polynomial coefficients, we find a P_0 and P_4 component of order unity and a substantial, negative P_2 component. However, because each point on the capsule's ablation surface integrates radiation flux over its 2π sky, the absorbed flux vs angle will be different from the source. For a small capsule, Green[2] showed that this integration causes the P_2 component to be attenuated by ~4, the P_4 component by 24, and higher modes by even more. Consequently, the major asymmetry in the absorbed flux is the P_2 asymmetry. For the capsule in the hohlraum of Fig. 1(a), that asymmetry has a *negative* P_2 component which, ultimately, produces a prolate implosion.

We can control the P_2 asymmetry by changing the pointing / aiming of the laser beams.[3] Figure 1(b) illustrates a situation where the beams are aimed to form hot spots much farther apart. Then, the collimated source flux has a substantial, *positive* P_2 component as well as P_0 and P_4 components of order unity. The 2π integration at the ablation surface causes the capsule absorbed flux to be dominated by a P_0 and positive P_2 component only, which ultimately produces an oblate implosion. Somewhere in between the situations shown in Figs. 1(a) and 1(b) is a beam pointing where the P_2 component of the source asymmetry vanishes [(Fig. 1(c)]. There, the ablation flux is dominated by the P_0 component and small, higher-order modes to produce an implosion that is substantially spherical.

Green's work on the attenuation of the P_2, P_4, and higher components was done for a small capsule inside a spherical hohlraum. Finite-size capsules and cylindrical hohlraums cause quantitative changes[4–6] but no significant qualitative changes.

Summary of Symmetry Experiments

Between 1987 and 1993, we performed a number of scaling experiments to examine our ability to understand the time-integrated P_2 asymmetry and to control it with beam pointing. In the most mature method of assessing the asymmetry, a pure-plastic capsule[7] filled with D_2 and a trace of Ar gas is placed in the center of a Nova hohlraum and is imploded by x-ray drive. Following the implosion is a bright flash of x rays produced by the hot, compressed fuel. At that time, we take pictures of the images formed by x rays viewed 90° off the polar axis through a hole in the side of the

[*] Los Alamos National Laboratory, Los Alamos, New Mexico

hohlraum. The resulting images show emission that is round, oblate, or prolate, depending on the beam pointing. (We discuss beam pointing later; also see Fig. 4 for an illustration.) Figure 2 shows some of our earliest images, from pure Au hohlraums irradiated by 1-ns flat-top pulses.

These first experiments demonstrated our ability to produce round, relatively symmetric implosions and confirmed that the long-wavelength mode dominated the hohlraum asymmetry. They also showed that we could control implosion asymmetry with beam pointing.[8] These experiments were done in early versions of our scale 1.0 hohlraums (1600-μm-i.d., ~2700-μm-long, 800-μm LEH diam) and used what has become our standard symmetry capsule—nominal dimensions of 440-μm-i.d., 55-μm-thick CH ablator / pusher, filled with 50 atm D_2 and 0.1% (at.%) Ar.

We have produced x-ray images of implosions using a number of gated and time-integrated diagnostics that have evolved over the years.[8–12] Numerical simulations of our standard symmetry capsule show good sensitivity to asymmetry. For pulse-shaped, convergence-10 implosions, we estimate that a 7%, fixed-in-time, pole-to-waist flux asymmetry will produce a 2:1 distortion of the x-ray image. We can measure distortions much closer to 1:1; therefore, we believe that the accuracy of our diagnostic technique is about 1%. That is, we can resolve equivalent, fixed-in-time asymmetries of ~1% pole-to-waist flux variation. A large body of evidence[13] indicates that these capsules, which operate at a pusher convergence of 7 to 10 depending on the pulse shape, do perform approximately as our model. There is good agreement between simulated and experimental capsule neutron yields, time-of-neutron production, and

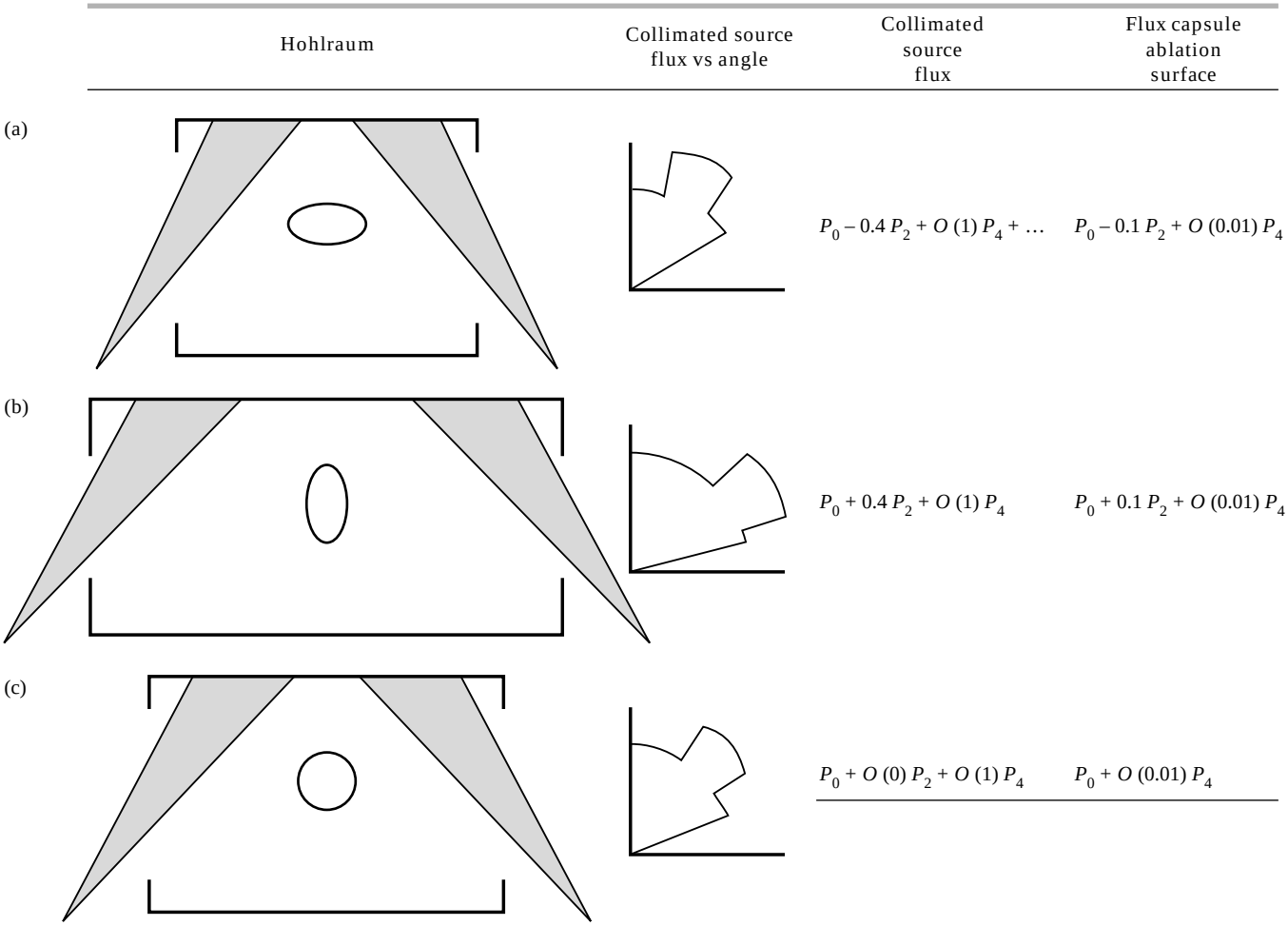

FIGURE 1. The collimated source flux vs angle viewed by a capsule in a laser-heated hohlraum has a substantial P_2, P_4, etc., component in addition to the P_0 component. Since each point on the ablation surface integrates over its 2π sky, the P_4, etc., components of drive asymmetry are heavily damped, leaving only the long-wavelength P_2 component as an asymmetry. This asymmetry can be controlled by beam pointing (see variations in a, b, and c for comparison). (20-03-0995-2123pb01)

image sizes. Spectroscopy confirms theoretical predictions that the x rays are principally produced by the Ar and that we are, in fact, imaging the fuel volume. Analysis of spectroscopy data and neutron data confirms calculated convergences. Reference 14 provides a comprehensive review of current drive asymmetry measurement techniques. Reference 15 provides a review of symmetry analysis.

The earliest experiments confirmed that the long-wavelength mode dominated and that it could be varied from shot to shot by changing the beam pointing in our out, as demonstrated in Fig. 2.[16] These results were largely qualitative. In 1990, we began producing systematic, quantitative symmetry studies.[14] The basic procedure of these experiments has been the same—for a given pulse shape and hohlraum type, we produce a symmetry scaling by varying the beam pointing while observing the resulting shapes of the capsules in self emission. Moving the beam pointing in tends to make a more prolate implosion; moving it out makes a more oblate implosion.

Between 1990 and 1993, we produced nine different symmetry scaling databases with the Nova laser using the three pulse shapes illustrated in Fig. 3. We have done three scalings with 1-ns flat-top pulses, five scalings with our 26-kJ, 2.2-ns, 3:1 contrast ratio pulse shape, called PS22, and one scaling with an 8:1 contrast ratio, 3.2-ns, 27-kJ pulse shape, called PS23. We have used these pulse shapes to irradiate both pure Au hohlraums and lined hohlraums as specified in the NTC. Lined hohlraums are Au hohlraums lined on the inside with a thin layer of either low-*Z* material (e.g., CH) or mid-*Z* material (e.g., Ni). We investigated lined hohlraums because we believe something like a liner to be necessary at larger, ignition scales.[17] For ignition hohlraums, we calculate that pure Au designs will fill with high-*Z* plasma. This causes the laser absorption region to move almost to the LEH, producing an unacceptably large radiation flux asymmetry on the capsule. Liners are one way to mitigate this effect by replacing the high-*Z* blowoff with low- or mid-*Z* blowoff.

With 1-ns flat-tops, we shot both pure Au and Ni-lined (1500-Å) Au hohlraums fixed in length at 2700 µm. We have also shot pure Au hohlraums where we varied the length of the hohlraum with the pointing so that the beams always cross in the plane of the LEH. We have done five scalings with PS22: fixed-length Au, Ni-lined Au, variable-length pure Au, Ni-lined Au, and CH-lined (0.75-µm) Au hohlraums. Our PS23 series used pure Au hohlraums that were open cylinders. As mentioned in the Introduction and in

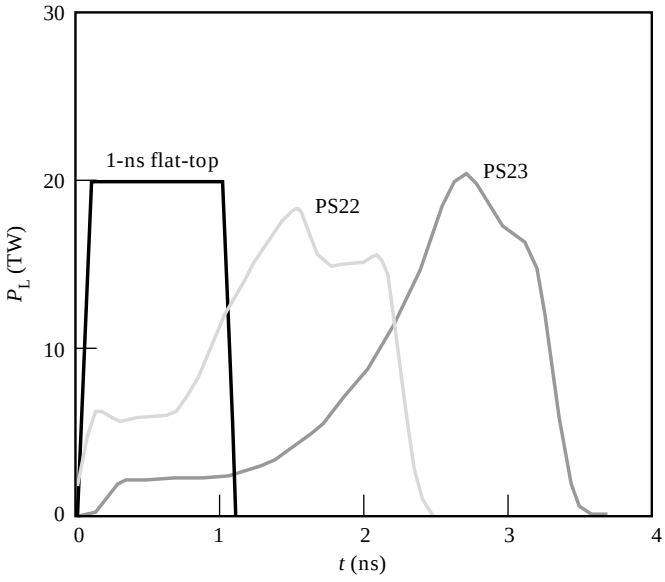

FIGURE 3. Symmetry scaling experiments using three different pulse shapes. (20-03-0995-2124pb01)

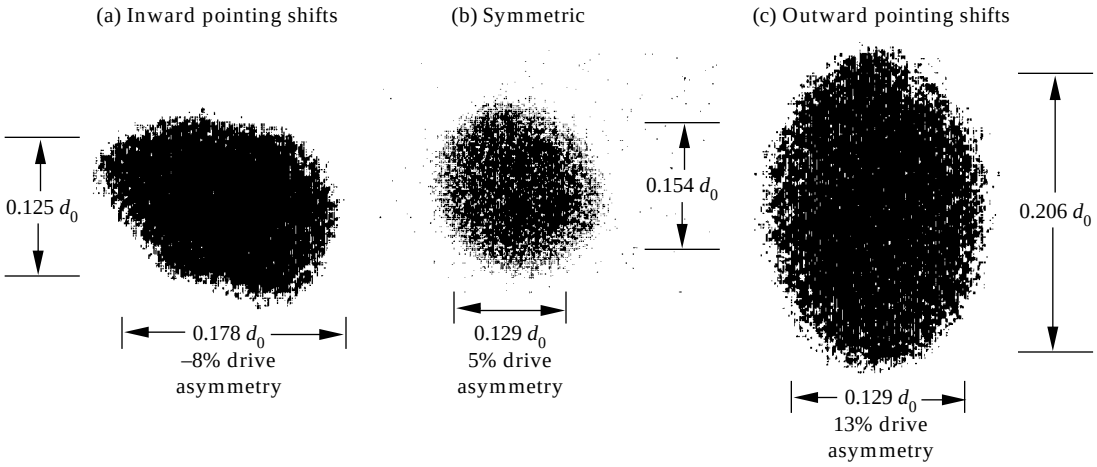

FIGURE 2. Capsule self-emission x-ray images from 1-ns experiments at three different beam pointing angles: (a) inward pointing, (b) symmetric, and (c) outward pointing. This illustration demonstrates that the fundamental hohlraum asymmetry is the long-wavelength P_2 asymmetry and can be controlled with beam pointing. (20-03-0995-2125pb01)

"Ignition Target Design for the National Ignition Facility" on p. 215, the NIF baseline target now uses an initial gas fill to displace the Au blowoff. Nova experiments with gas-filled hohlraums have also demonstrated control of symmetry. However, these experiments are still in progress and therefore will be reported at a later time.

Modeling the Experiments

We use our 2-D LASNEX computer code[18] to perform detailed modeling of these experiments. Figure 4 is a cut-away, at $t = 0$, from a simulation of a hohlraum containing a pure-plastic capsule that is irradiated by a "realistic" 2-D representation of a three-dimensional (3-D) Nova laser beam.[19] The wall materials, laser power vs time, etc., of a given simulation are our best estimate of what was used in the experiments we are trying to model. To model a given symmetry scaling, we performed a number of simulations with different beam pointings. At stagnation, our simulated capsules, like real capsules, produce a burst of x rays that can be imaged. A post-processor simulates the actual x-ray diagnostics, producing synthetic images that vary with pointing from oblate or prolate (like the experiment). The ratio of the image's full-width at half maximum (FWHM), perpendicular to the polar axis to the FWHM along the polar axis is the "distortion," the quantity we vary with pointing and compare with experiment.

Our calculations start off fully Lagrangian (matter is fixed in the zones of a moving mesh). Later in time, after a considerable amount of blowoff has filled the hohlraum, we perform a major rezone and change our numerical scheme. The main part of the hohlraum becomes Eulerian (matter flows through a fixed mesh), allowing the calculation to run in spite of the large sheer flows. Most of the capsule, however, remains Lagrangian—the accepted procedure for modeling nearly spherical implosions. We interface the Eulerian and Lagrangian regions with a stretching region that maintains equal-ratio zoning—a hybrid mesh that has matter flowing through it while moving slowly. Using three numerical schemes in the same calculation allows us to simulate both the main hohlraum and the capsule with the most appropriate numerical technique.

To provide an example of how we model a given scaling, consider a series of shots with Au hohlraums (1600-μm-diam with 1200-μm-diam LEHs lined with 1500-Å Ni). In this series, to keep LEH effects approximately the same for all pointings we varied the hohlraum length with pointing so that the beams always crossed in the plane of the LEH. We used the nominal capsules, defined earlier, and irradiated these targets with PS22. The self-emission x-ray images from the imploded capsule were the key observations made on this (and all other) scaling series. Our x-ray diagnostics were time-resolved (~100-ps frame time) and time-integrated cameras filtered to measure emission >3 keV from the Ar fuel dopant.

Figure 5 displays the results of the PS22 series experimental scaling and compares it with our model. The solid circles are distortions from our experiments as a function of beam pointing. The horizontal error bar shows an estimated ±50-μm systematic uncertainty in the absolute pointing of the beams (the relative shot-to-shot pointing jitter is believed to be considerably smaller than this). The open circles are modeling distortions. Both experiment and modeling agree that we can control Nova symmetry by varying the beam

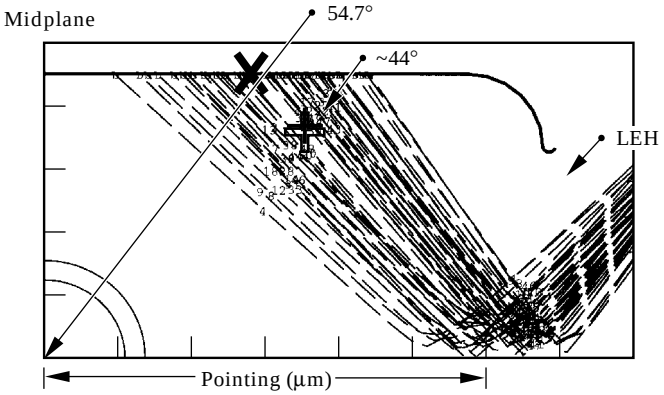

FIGURE 4. Cutaway at $t = 0$ from a 2-D simulation of a hohlraum containing a pure-plastic capsule with a realistic representation of Nova's beams. The calculation is cylindrically symmetric around the horizontal axis and left-right symmetric across the midplane. The beams enter through LEHs at the ends of the hohlraum. Pointing is the distance between the midplane and where the beams cross (i.e., the reflection off the horizontal, rotational axis of symmetry). The "X" and "+" show the center of emissivity early in time at 1.4 ns, respectively. (20-03-0995-2126pb01)

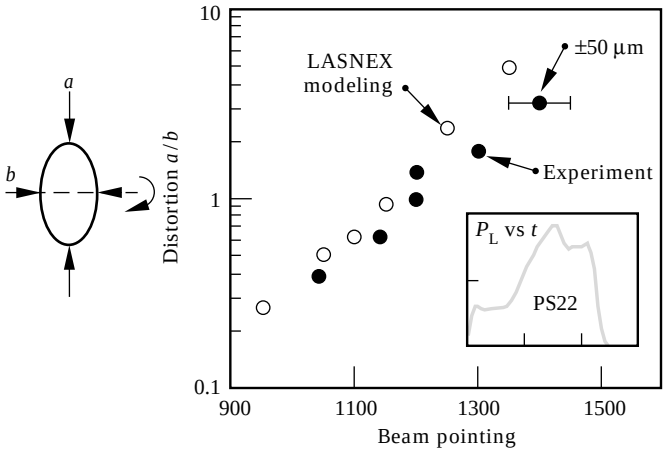

FIGURE 5. Capsule image distortion vs pointing from a series using Ni-lined hohlraums irradiated by PS22. (Inset: Relative laser power vs time for PS22.). Experimental uncertainty is ±50 μm. (20-03-0995-2127pb01)

pointing. Also, they both produce about the same pointing of best symmetry (~1200 ± 50 μm in experiment and ~1150 μm in modeling).

The pointing of best symmetry changes as we vary the pulse shape. For example, another scaling series used fixed length (2700-μm), Ni-lined Au hohlraums irradiated with 1-ns flat-top pulses. In this series, both modeling and experiment also verified that we can control Nova symmetry by varying the beam pointing. However, for this pulse shape, the pointing of best symmetry is about 100 μm outward from the best pointing found in the PS22 series. For this 1-ns experiment, the pointing of best symmetry is ~1320 ± 50 μm in experiment and ~1250 μm in modeling.

Scaling of the Pointing of Best Symmetry

Figure 6 summarizes our ability to estimate the pointing of best symmetry over our nine symmetry scaling databases. It plots the pointing of best symmetry inferred from experiment against that of our integrated LASNEX simulations. Overall, we find the agreement to be very satisfactory. The vertical error bars in this plot indicate only the uncertainty in the pointing of best symmetry extracted from each experimental dataset, using the nominal pointing. The error bars do not include the systematic uncertainty in Nova's absolute pointing (~50 μm), which would allow all the points to be moved as a group, either up (toward poorer agreement) or down (better agreement). Regardless of systematic differences, the most significant and apparent feature of the plot is this: *the longer the pulse shape, the farther in we must point the beams to get good symmetry.*

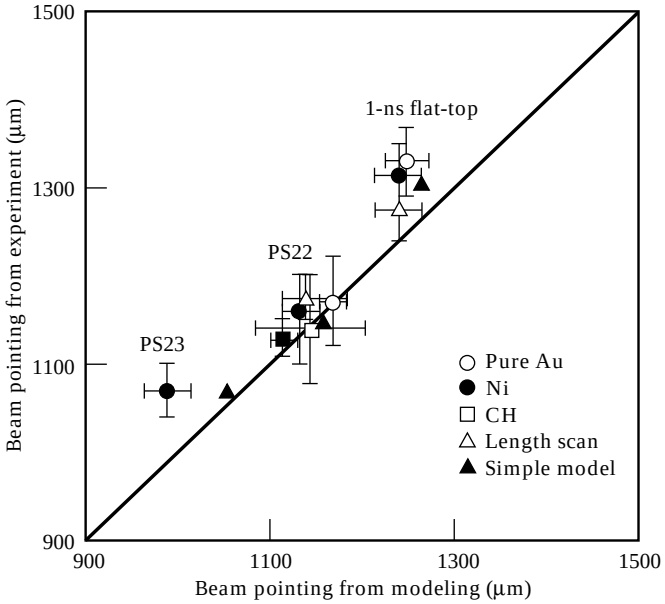

FIGURE 6. Pointing of best symmetry in our experiment vs pointing of best symmetry from our modeling. The longer the pulse shape, the farther in the beams need to be moved to get good symmetry. The solid triangles plot the pointing to compare with Eq. (2).
(20-03-0995-2128pb01)

The reason for this is found in the basic principles of symmetry scaling in Nova-type hohlraums. First, there are hot, laser-produced emission rings that migrate toward a smaller polar angle (when viewed from the capsule position) because of bulk plasma evolution. We refer to this migration as "spot motion." Second, there is also an "optimal" polar angle for the rings where time-integrated pole-flux equals equator flux (~48° for these hohlraums). Third, to get good symmetry we must point the beams so the emission rings pass through 48° when we deliver ~50% of a shape's useful energy. Since spot velocity is weakly dependent on laser intensity, we move the beams farther inward with longer pulses.

In our simulations, there are three components to spot motion. First, dense plasma evolution from the cylindrical walls causes the laser deposition region to move inward and, because of the beam geometry, toward the LEH. Second, there is a refractive component off plasma that accumulates on axis. Third, there can be a low-intensity volume emission when Au blowoff fills the hohlraum, pulling the average center of emissivity farther down from the walls. In our simulations, which use a nonLTE, average-atom atomic physics model,[20] the Au blowoff is optically thin to thermal radiation. Consequently, volume absorption does not play a significant role in determining the capsule flux.

To see how spot motion can cause the scaling shown in Fig. 6, first recall that the fundamental asymmetry in a left-right symmetric, Nova-like hohlraum is a long-wavelength, pole-to-waist flux variation that varies like the P_2 Legendre polynomial.[2] Whether the asymmetry is pole high or equator high depends on the polar angle to the center of the laser-produced, x-ray emission ring. In an idealized hohlraum without LEHs and with otherwise uniform walls, the drive asymmetry will clearly be pole high when the emission ring is at a very small polar angle and equator high when the emission ring is near the midplane of the hohlraum. Somewhere in between, the pole and equator fluxes will be equal. In a spherical hohlraum, the P_2 component of capsule flux vanishes when the P_2 component of the source flux is zero.[2] This occurs when the "center of emissivity" of the emission ring is at the polar angle where P_2 is zero, 54.7°. For larger angles, the flux onto the capsule will be equator high, and for smaller angles, pole high.

An LEH modifies this description quantitatively, but not qualitatively. To compensate for the lack of wall radiation from the LEH, the angle to the center of

emissivity in a spherical hohlraum must be smaller than 54.7° for the net P_2 component to vanish. Exactly how much smaller than 54.7° is a function of both the emission-ring to background-wall intensity ratio and the LEH size. For example, the angle where the P_2 component of the source vanishes is about 44° in an idealized spherical hohlraum with wall and LEH areas the same as ours and a wall albedo (which determines the emission-ring to background-wall intensity ratio) of ~0.7. This albedo is typical of a rising, nanosecond-scale pulse shape. In our more detailed LASNEX simulations, we find the pole:waist fluxes are balanced when the center of emissivity is at ~48°. These simulations include higher *l*-mode components, volume emission, and mode-coupling due to having a sphere inside a cylinder.

With this background, we can simply interpret features found in our LASNEX modeling. Figure 7 plots ratios of capsule ablation pressure at the pole to that at the equator vs time in pure Au hohlraums near the pointing of best symmetry for each pulse shape. Early in time, the ablation pressure is equator high. Later in time, the pressure is pole high. Analysis of our simulations indicates that this time-dependent asymmetry is produced mainly by spot motion. As shown in Fig. 4, the angle to the center of the beam at $t = 0$ for PS22 is >54.7°. Quantitative analysis shows the center of emissivity to be located at the "X" in Fig. 4 at ~57°. The simple symmetry arguments lead us to expect the drive to be equator high, as Fig. 7 shows in the early PS22 curve. By 1.4 ns, spot motion has caused the center of emissivity to move to the "+" in Fig. 4 to ~44°. There, the ablation pressure ratio has become about 10% pole high.

Spot motion, the migration of the radiation production region to smaller polar angles, causes a simulated Nova-type hohlraum to have the characteristic equator-high to pole-high asymmetry swing shown in Fig. 7. For all three pulse shapes, we find that near the pointing of best symmetry the center of emissivity sweeps through the "optimal angle" (where pole pressure = equator pressure, ~48° for these hohlraums) when ~50% of a shape's useful energy has been delivered. This 50% value makes sense. If the pressures were equal when a very different fraction of energy was delivered, the implosion would be dominated by either pole-high or equator-high flux and would be obviously distorted. Therefore, since spot velocity depends weakly on laser power P_L, longer pulses need more inward pointing for best symmetry because $t_{50\%}$, the time to deliver ~50% of the energy, is longer, leading to more spot motion.

LASNEX simulations show spot-angular velocity to be very weakly dependent on P_L. Figure 8 is a plot of the angle to the center of emissivity vs time for our three pulse shapes (refer to Fig. 3). Over the period when the first 50% of the laser energy is delivered, the angular velocity $d\theta/dt$ of the center of emissivity in our simulations increases only as the logarithm of P_L (measured in TW) closely following

$$\frac{d\theta}{dt} = \frac{6^\circ}{\text{ns}} + \frac{3.9^\circ}{\text{ns}}\left(\log_{10} P_L\right). \quad (1)$$

We can couple this expression for spot motion with the need to have the center of emissivity at ~48° when ~50% of the laser energy has been delivered to produce

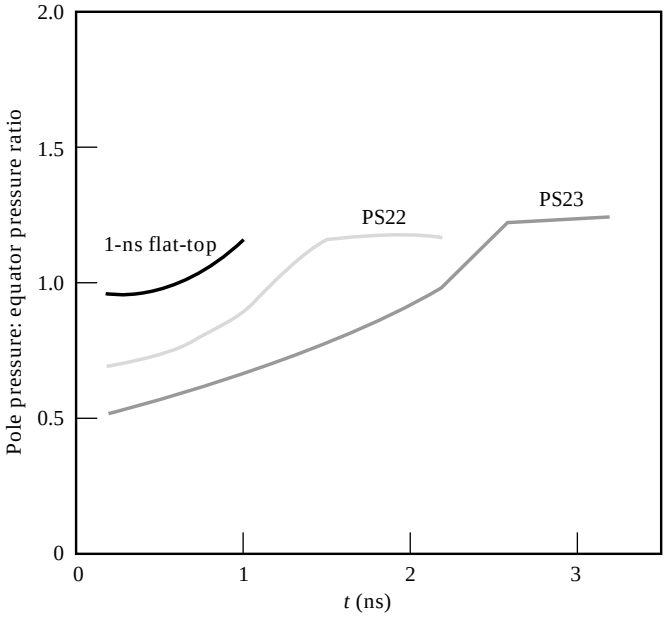

FIGURE 7. Ratio of capsule ablation pressure at the pole to the ablation pressure at the equator vs time for our three pulse shapes. (20-03-0995-2129pb01)

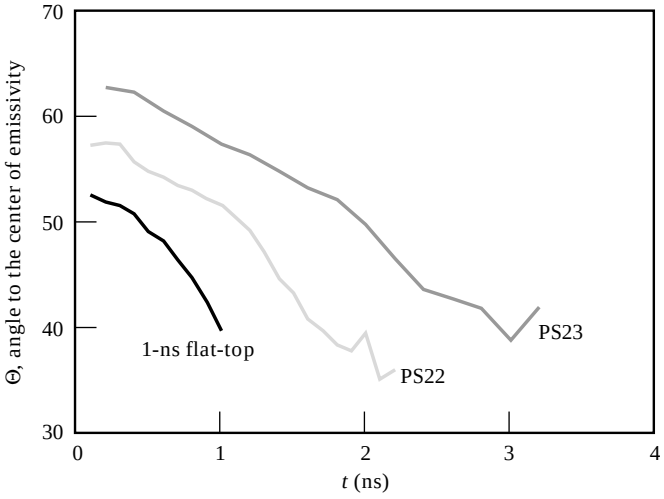

FIGURE 8. Angle to the center of emissivity vs time in our LASNEX simulations of the three pulse shapes. The angular velocity during the period when the first half of a pulse shape's energy is delivered varies slowly with laser intensity. (20-03-0995-2130pb01)

a simple expression for the pointing of best symmetry

$$\text{best pointing} = 671\ \mu\text{m} + \left[\frac{800\ \mu\text{m}}{\tan\left(48^\circ + \frac{d\theta}{dt} \times t_{50\%}\right)}\right]. \quad (2)$$

This expression is for our standard 800-μm radius hohlraums and Nova's 50° half-cone angle. The results of this very simple model are plotted as the filled triangles in Fig. 6 and also agree well with our database.

Spot Motion

Since 1986, we have performed separate experiments to observe laser-produced x-ray emission spots and their migration.[21] We cut an 800 μm × 1200 μm rectangular observation port into the side of a hohlraum through which we take time-resolved x-ray images of the opposite wall with a three-channel x-ray framing camera that takes snapshots at four different times.[22] Our field of view includes the initial spot of a beam as well as some of the surrounding region. Figure 9 shows the images from the 450-eV channel for a pure Au PS22 experiment. Qualitatively, these images verify that there are spots and that they do migrate toward the LEH. Quantitatively, we analyze these images to find the center of emission, within the port's field of view, at various times. For comparison, we quantitatively analyze LASNEX simulations of the experiment with a postprocessor that mimics the imaging diagnostic and the analysis. Figure 10 shows such a comparison, plotting the position of the center of emission for the 450-eV channel from pure Au PS22 simulations and experiments. The good comparison with LASNEX shows that we can calculate the component of spot motion observed—the component along the hohlraum wall. The data from four different shots show that the motion is reproducible. Reproducible spot motion has also been indirectly corroborated by Precision Nova shots that produced nearly identical capsule shapes and performances for five PS22 shots at one pointing and four shots at another (see Fig. 11).

Time-Dependent Asymmetry

An essential feature of theory and simulation is that

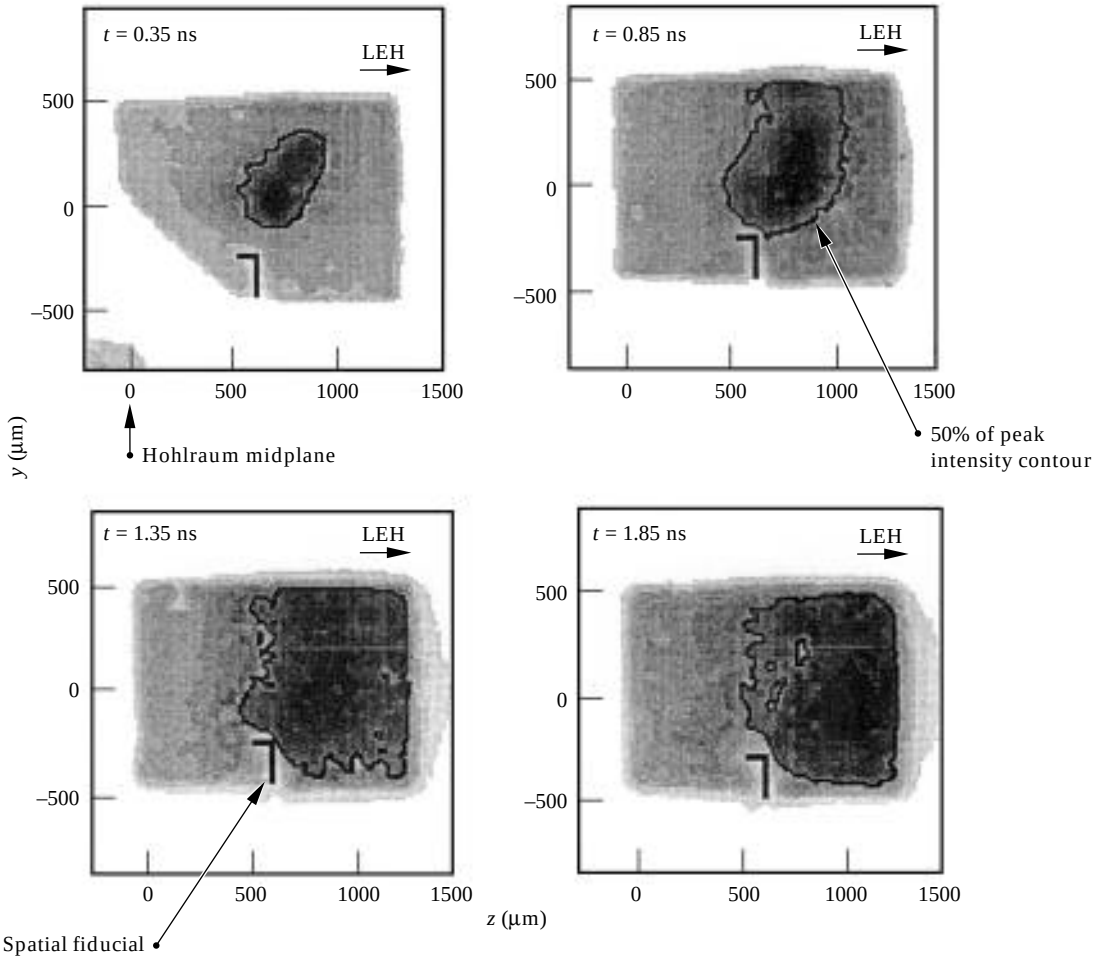

FIGURE 9. 450-eV images of spots inside a pure Au hohlraum during a PS22 experiment. The black "7" is a spatial fiducial. These images show a well defined soft x-ray spot that moves toward the LEH. (20-03-0995-2131pb01)

the asymmetry in a Nova-like hohlraum will vary over time. This causes the variation in the pole-to-equator ablation pressure ratio shown in Fig. 7. Time-dependent asymmetry results both from changing hot spot to background-wall ratio and from spot motion.

Experiments provide persuasive evidence that the time-dependent asymmetry in Nova hohlraums is about as we expect. The hot spot to background-wall ratio is largely determined by the albedo of the Au wall. Separate measurements of Au wall losses[23] indicate that LASNEX accurately estimates Au albedo at standard Nova temperatures (~220 eV). The spot-motion experiments described earlier are qualitatively and quantitatively close to what we expect. Finally, the changes in the pointing of best symmetry (Fig. 6) with pulse shape indicate that the variation in flux at the capsule is qualitatively what we expect—the asymmetry goes from waist high early in time to pole high later in time.

To understand this final point, consider PS22 at its experimental pointing of best symmetry, 1200 µm. According to Fig. 7, the first 1 ns of PS22 should provide a waist-high radiation flux that drives a prolate implosion. However, our 1-ns implosions at 1200 µm are prolate, showing that at ~20 TW the first 1 ns of drive at this pointing is predominantly waist high. Because the first nanosecond of PS22 is actually at much lower power, ~6 TW, we expect it to also be predominantly waist high since there is (slightly) less spot motion at lower power, and spot motion is needed to get into the pole-high regime. Moreover, we argue that the entire first nanosecond should be waist high. If the PS22 flux did change to pole high before 1 ns, so much of the PS22 energy would be generating pole-high flux that 1200 µm would not be PS22's pointing of best symmetry. Continuing the argument, since the early part of PS22 is waist high, some latter part of PS22 must be pole-high to compensate for this early-time asymmetry. Consequently, the scaling of the pointing of best symmetry with pulse length (shown in Fig. 6) is evidence that the time-dependent asymmetry goes from waist-high early in time to pole-high later in time, therefore corroborating the qualitative behavior of Fig. 7.

Other experiments are ongoing to more directly measure the time-dependent asymmetry in Nova hohlraums. One approach, proposed by Wilson,[24] uses the full pulse with a series of capsules designed to implode at

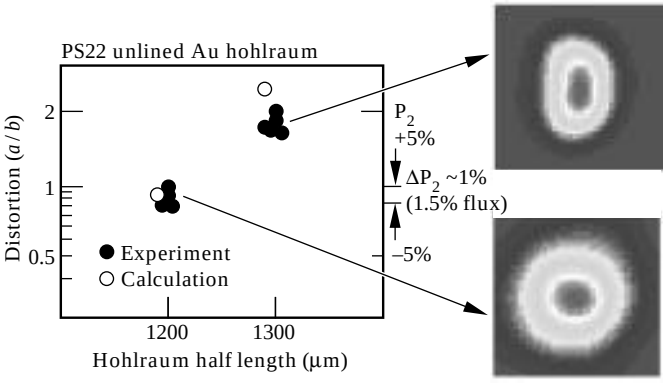

FIGURE 11. Precision Nova implosions have shown excellent reproducibility of symmetry. (08-00-1293-4416pb01)

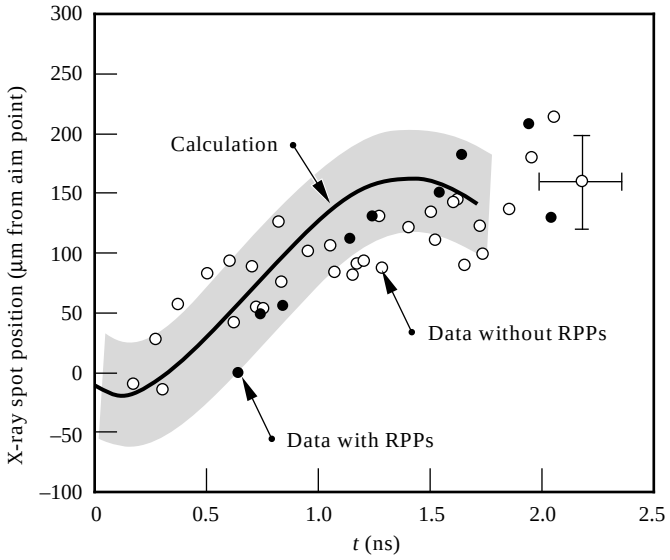

FIGURE 10. Distance from the hohlraum midplane to the center of emission at $h\nu \approx 450$ eV, vs time in a pure Au hohlraum irradiated by PS22. We observe spots that migrate about as expected from simulations. (20-03-0995-2132pb01)

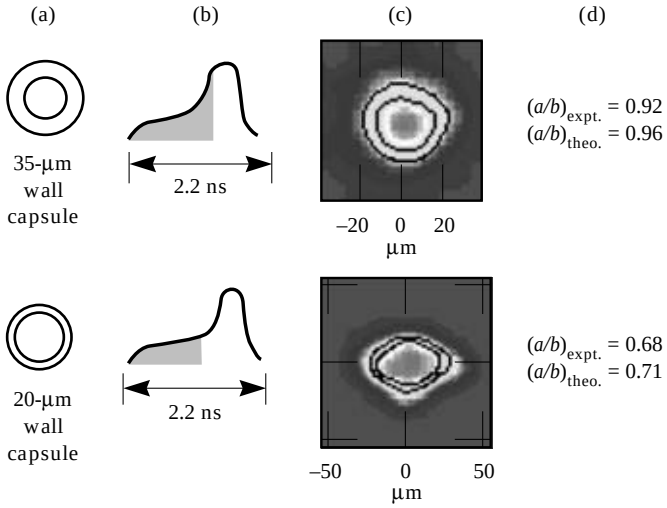

FIGURE 12. Data from PS22 using the variation in implosion time of capsules with different wall thickness: (a) initial capsule configuration; (b) shaded portion of the drive represents the effective sampling interval for the implosion for the two cases; (c) implosion image data taken orthogonal to the hohlraum axis; (d) comparison of the measured capsule eccentricity with the calculated value. (02-08-1094-3596pb03)

different times during the pulse. This is accomplished by keeping the capsule's i.d. approximately fixed and thinning the ablator to significantly less than its standard 55-μm thickness. The thinnest capsules view only the early-time asymmetry, and a record of the evolution of asymmetry can be obtained. Figure 12 shows results of this technique for PS22 and Au hohlraums.[25] Another technique replaces the capsule with a uniform sphere of material. The x-ray flux in the hohlraum will drive a shock into this material, which can be imaged by x-ray backlighting (see Fig. 13). Distortion of the shock front is approximately related to the drive pressure nonuniformity by

$$\frac{d}{dt}\left(r_{\text{equator}} - r_{\text{pole}}\right) \approx \frac{1}{2}\sqrt{\frac{\bar{P}}{\rho}}\left(\frac{P_{\text{pole}}}{P_{\text{equator}}} - 1\right) \quad . \tag{3}$$

For PS22, Fig. 13 shows the calculated ratio of $P_{\text{pole}}/P_{\text{equator}}$, which can then be compared with the measurement. The average pressure $\bar{P}$ can be obtained from the shock velocity. Figure 14 shows the results from a Nova experiment.[26] In this figure, A_2 is the second Legendre coefficient of the position of the shock trajectory, and A_0 is the average distance moved by the shock. The numerical calculation and the data are in agreement for this experiment. Calculations[27] show that, with the current resolution of about 2 μm in the shock position, time variations in NIF target fluxes can be obtained to about 2%.

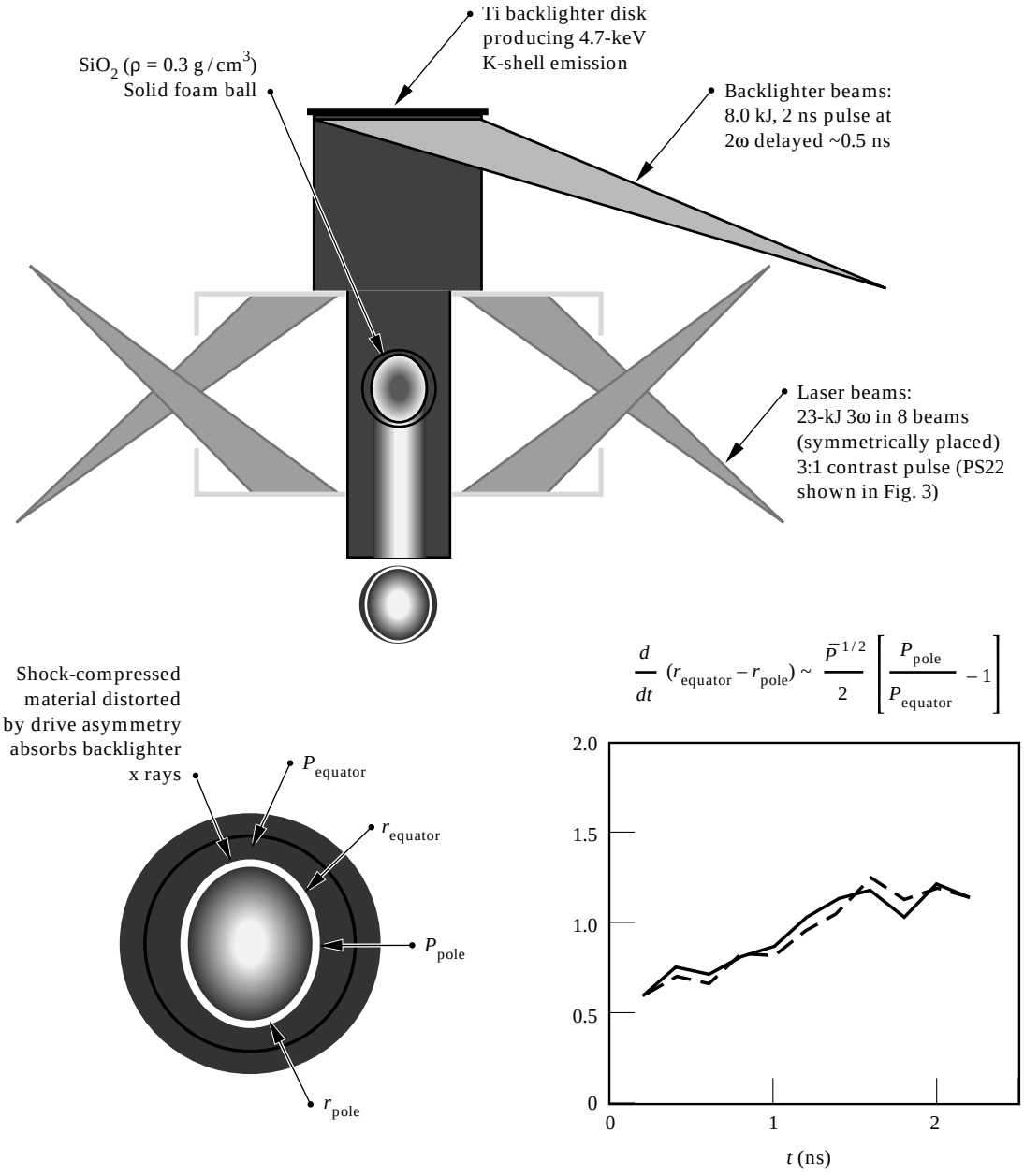

FIGURE 13. X-ray radiography can be used to infer time-dependent asymmetry from imaged shock distortion.
(50-04-1093-3882Apb03)

The Role of the LEH

Figure 15 summarizes the main effect an LEH can have on simulated beam propagation. It shows rays and electron density contours 2 ns into PS22. For nominal pointing shown in Fig. 15(a), when Nova's beams initially cross in the plane of the LEH, all rays are far from the blowoff that expands from the lip. Consequently, they are unaffected by LEH blowoff. However, Fig. 15(b) shows what can happen if we move the beams farther inward, close to the LEH. The part of the beam closest to the LEH intersects blowoff dense enough to refract those rays downward. Since these rays otherwise strike closest to the midplane of the hohlraum, the effect of the refraction is to shift the center of deposition toward the LEH. This shifts the asymmetry back in the pole-high direction. Note, however, that even when there is considerable interaction between the rays and the lip blowoff, the density distributions shown in Fig. 15 are very similar. This implies that there is no significant amount of additional blowoff produced by the interaction. These LEH results basically reproduce earlier findings of Lasinski,[28] who modelled an isolated LEH as a thin bracelet of material subjected to both a radiation source and a laser source. Her modeling agrees quite well with available data on radiation-driven LEH hydrodynamics.[28,29]

Modeling and experiment show that bringing the beam too close to the LEH can cause different symmetry behavior, as shown in Fig. 15(b). Consider a case where the LEH should have no effect—the distortion vs pointing scaling shown earlier in Fig. 5. This is the Ni-lined, PS22 scaling where the hohlraum length changed with pointing. In the experiments of Fig. 5, we expect the laser-LEH interaction to always be the nominal situation shown in Fig. 15(a). The straight-line scaling of Fig. 5 indicates there is no obviously "different" symmetry regime at inner pointing.

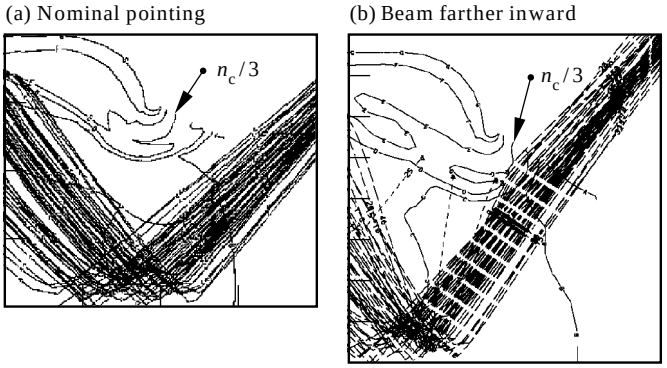

FIGURE 15. Simulated laser rays and density contours 2 ns into PS22 in a Ni-lined hohlraum. (a) With nominal pointing the laser is sufficiently far from the cylindrically expanding blowoff from the LEH lip that there is no significant interaction. (b) If the beam is moved too far inward, it can intercept relatively dense plasma and be partially refracted. (20-03-0995-2133pb01))

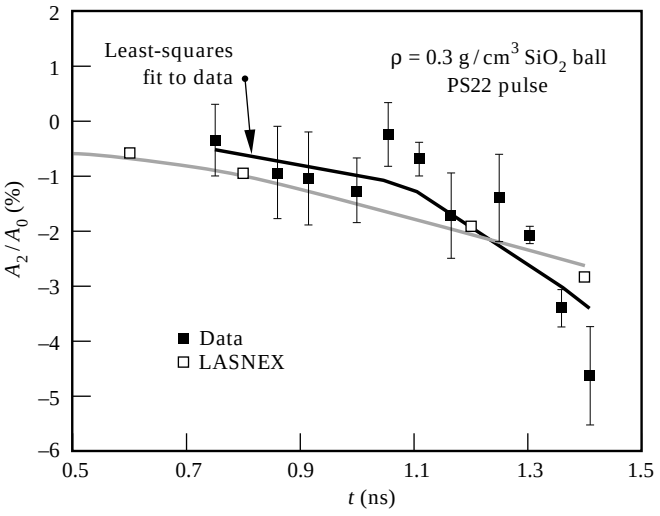

FIGURE 14. The foam witness ball technique can measure pressure asymmetries with nearly 10% accuracy on Nova. A_2 is the second Legendre coefficient of the shock trajectory. A_0 is the average shock position. (50-04-1093-3891Apb02)

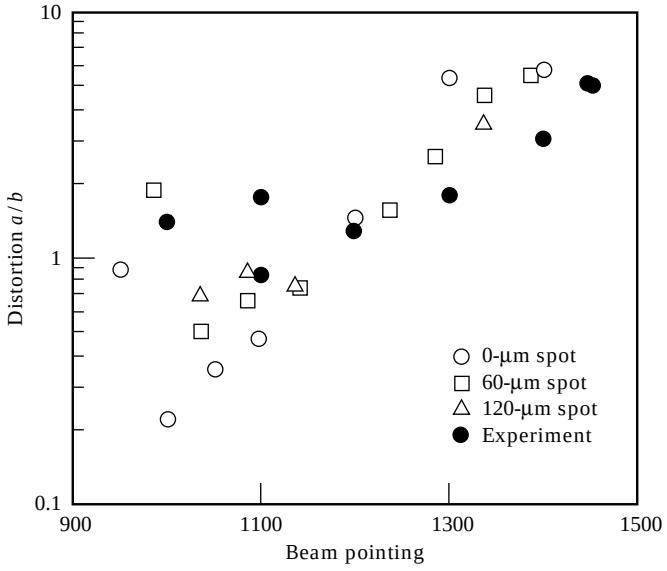

FIGURE 16. Symmetry scaling experiments (solid circles) in fixed length hohlraums show a "different" behavior at inner pointing than experiments where we vary the length with the pointing (see Fig. 5). This trend is reproduced in our simulations where we see it is due to refraction such as shown in Fig. 11(b). (20-03-0995-2134pb01))

Figure 16 plots simulations and experiments where the symmetry at inner pointing is different, showing a Ni-lined, PS22 scaling performed with fixed-length (2700-μm) hohlraums. At inner pointing, the beams approach the LEH and can be refracted. Comparison with Fig. 5 shows a different behavior at inner pointing.

Similar to the experiment, the LASNEX modeling shows a different symmetry regime can be found at inner pointing with fixed-length hohlraums. This is due to refraction by LEH blowoff. The size of the effect depends on the details of the beams. We studied this effect with simulations of three different realizations of Nova's beams, all of them using the 3-D geometric optics raytrace algorithm devised by Friedman.[19] The nominal beam representation has, at best focus, a 60-μm-diam, 1-sigma circle of confusion. This produces the rays shown in Figs. 4 and 15 and is a best-guess lower bound on the wings of Nova's beams. This beam representation produces the open squares of Fig. 16.

In addition to the 60-μm circle of confusion, we simulated beams with 120-μm-diam circles of confusion (upper bound to Nova) and 0-μm-diam circles of confusion (better than diffraction limited). The 0-μm circle of confusion beams (open circles of Fig. 16) cause no break in the distortion vs pointing scaling until the beam is so far in that it strikes the LEH. The 120-μm circle of confusion (open triangles of Fig. 16) representation shows somewhat more of an inner pointing refractive effect than the nominal beam representation.

The scalings of Fig. 16, together with those of Fig. 5, are evidence that the LEH can have an effect on symmetry. They also indicate that LASNEX can estimate when, and roughly how much, an LEH will have a major effect on hohlraum symmetry.

Summary

Our 2-D LASNEX simulations of Nova's nine symmetry scaling databases reproduce the fundamental features seen in the experiments. In particular, we predict how we must change Nova's beam pointing to achieve best symmetry with various pulse shapes. Analysis indicates that the need to change pointing with different pulse shapes is a result of spot motion. Complementing direct-symmetry measurements, we have also observed and modelled hot spots in hohlraums. We find hot-spot motion to be real, reproducible, and very close to what we expect from LASNEX. These measurements also indicate that time-dependent asymmetry in the Nova hohlraums behave close to our modeling. Experiments and modeling also indicate that we estimate when, and roughly how much effect, an LEH will have on hohlraum symmetry.

Notes and References

1. *Laser Program Annual Report–1979*, 2-77 to 2-88, Lawrence Livermore National Laboratory, Livermore, CA, UCRL-50055-79 (1979, report SRD); *Laser Program Annual Report–1980*, 2-10 to 2-22, Lawrence Livermore National Laboratory, Livermore, CA, UCRL-50055-80 (1980, report SRD).
2. J. Green, Research and Development Associates, private communication (1980); M. Murakami and K. Nishihara, *Jpn. J. Appl. Phys.* 25, 242 (1986); A. Caruso, *Internal Confinement Fusion* (Proc. Course and Workshop, Varenna, 1988), *Casa Editrice Compositori*, Bologna (1988) 139.
3. *Laser Program Annual Report–1984*, 2–13, Lawrence Livermore National Laboratory, Livermore, CA, UCRL-50055-84, M-3679, C-72 (December 1985, report SRD).
4. S. W. Haan, "Radiation Transport Between Concentric Spheres," Lawrence Livermore National Laboratory, Livermore, CA, UCRL-ID-118152 (1994); J. Green, Research and Development Associates, private communication (1983).
5. *Laser Program Annual Report–1983*, 2–21, Lawrence Livermore National Laboratory, Livermore, CA, UCRL-50055-83 M3679, C-72 (September 1984, report SRD).
6. *Laser Program Annual Report–1985*, 30–31, Lawrence Livermore National Laboratory, Livermore, CA, UCRL-50055-85 M3679, C-72 (September 1986, report SRD).
7. A. Burnham, J. Grenz, and E. Lilley, *J. Vac. Sci. Technol. A* 5 (6), 3417 (1987).
8. *Laser Program Annual Report 1986/87*, 2–50 to 2–54 and 4–25 to 4–34, Lawrence Livermore National Laboratory, Livermore, CA, UCRL-50055-86/87 (1988, Title U, report SRD); *Laser Program Annual Report: Target Design 1988*, 51–75, LLNL, XDIV-90-0054 (Title U, report SRD); *ICF Program Annual Report 1988/89 (U)*, 192, LLNL, UCRL-LR-116901-88/89 (report SRD).
9. D. B. Ress, Lawrence Livermore National Laboratory, Livermore, CA, private communication (1995).
10. A. Hauer, Los Alamos National Laboratory, Los Alamos, NM, private communication (1992).
11. J. D. Kilkenny P. Bell, R. Hanks, G. Power, R. E. Turner, and J. Wiedwald, *Rev. Sc. Instrum.* 59 1793 (1988).
12. A. Hauer, Los Alamos National Laboratory, Los Alamos, NM, private communication (1995).
13. *ICF Program Annual Report 1988/89 (U)*, 9, Lawrence Livermore National Laboratory, Livermore, CA, UCRL-LR-116901-88/89 (report SRD).
14. A. Hauer, et. al., *Rev. Sci. Instrum* 66(1), 672 (1995).
15. L. J. Suter, A. A. Hauer, L. V. Powers, D. B. Ress, et al., *Phys. Rev. Lett.* 73(17), 2328 (1994).
16. R. E. Turner and L. J. Suter, *Bull. Am. Phys. Soc.* 1 (1988); Y. Kato, et. al., *Proc. 13th Int'l Conf. Plasma Physics and Controlled Nuclear Fusion Research*, Washington, DC, 1990.
17. *Laser Program Annual Report: Target Design 1988 (U)*, 223, Lawrence Livermore National Laboratory, Livermore, CA, XDIV-90-0054 (May 1990, report SRD).
18. G. Zimmerman and W. Kruer, *Comments Plasma Phys. Controlled Fusion* 2, 85 (1975).
19. A. Friedman, *Laser Program Annual Report 83*, 3–51, Lawrence Livermore National Laboratory, Livermore, CA, UCRL-50021-83 (1983).
20. D. E. Post, R. V. Jensen, C. B. Tarter, W. H. Grasberger, and W. A. Lokke, *Atomic Data and Nuclear Tables* 20(5) (Nov 1977); G. B. Zimmerman and R. M. More, *JQSRT* 23, 517 (1980).
21. D. Ress, L. V. Powers, L. J. Suter, R. J. Wallace, and F. Ze, *Bull.*

Am. Phys. Soc. 38, 1885 (1993); L. V. Powers, D. B. Ress, L. J. Suter, and F. Ze, *Defense Research Review* 6(10), (1994, report SRD).
22. G. Glendinning, Lawrence Livermore National Laboratory, Livermore, CA, private communication (1995).
23. J. L. Porter, T. J. Orzechowski, M. D. Rosen, A. R. Thiessen, et al., *ICF Quarterly Report* 4(4), 125–131, Lawrence Livermore National Laboratory, Livermore, CA UCRL-LR-105821-94-4 (1994).
24. D. Wilson, Los Alamos National Laboratory, Los Alamos, NM, private communication (1992).
25. A. A. Hauer, "X-Ray Driven Implosions in Laser Heated Hohlraums," *Laser Plasma Interactions*, Eds., M. Hooper and A. Cairns (Redwood Burn, Trowbridge, England, 1995), vol, 5, pp. 5–24.
26. P. Amendt, S. G. Glendinning, B. A. Hammel, R. G. Hay, and L. G. Suter, *Rev. Sci. Instrum*. 66(1), 785 (1995).
27. P. Amendt, Lawrence Livermore National Laboratory, Livermore, CA, private communication (1995).
28. B. F. Lasinski, Lawrence Livermore National Laboratory, Livermore, CA, private communication (1990).
29. C. Gomez, Los Alamos National Laboratory, Los Alamos, NM, private communication (1991).